doi:10.1246/cl.2010.532
Published on the web April 24, 2010

Highlight Review

Random Dispersion of Metal Nanoparticles Can Form a Laser Cavity

Shunsuke Murai, Koji Fujita,* Xiangeng Meng, and Katsuhisa Tanaka*

(Received March 1, 2010; CL-108004)

Abstract

Metal nanoparticles are efficient scatterers for light at around the frequency of localized surface plasmon resonance. By randomly dispersing such strong scatterers in a gain material, a laser system is achieved. Multiple scattering leads to an optical feedback that selects lasing modes. This type of laser is called random laser and has been developed using dielectric scatterers. This article highlights the application of metal nanoparticles to random laser and emphasizes the advantages of metallic scatterers compared to dielectric scatterers.

♦ Introduction

Metal nanoparticles exhibit properties different than those of bulk counterparts. One distinct difference is the behavior of plasmon, which is a collective oscillation of conducting electrons with respect to the positively charged metal ions of which the lattice is composed. While bulk plasmon cannot be directly excited by light illumination, the polarization developed by charge oscillation on particle surfaces provides an effective restoring force that yields conditions for light coupling to plasmon.[1] When the eigenfrequency of the surface polarization matches the frequency of incident light, a resonance, termed localized surface plasmon resonance (LSPR), takes place on a particle. Through LSPR, electromagnetic oscillation is converted into plasmonic oscillation and confined in nanoscale, which brings about an associated enhancement of electromagnetic field around the particle. These interesting phenomena make the metal nanoparticle an important player in plasmonics, a branch of photonics based on surface plasmon. Potential applications in plasmonics include surface-enhanced Raman scattering, bio-chemical sensing, drug targets, solar cells, and even cancer therapy.[2]

In this highlight review, we focus on scattering properties of metal nanoparticles, one of the notable features related to LSPR, and describe the application of nanoparticles as components of a laser cavity. While a Fabry–Pérot cavity confines light by a pair of facing mirrors, randomly dispersed particles can trap light by multiple scattering and interference. Lasers with this type of cavity are called random lasers and have been developed mainly using dielectric scatterers. In the following sections, we first describe scattering properties of a metal nanoparticle, emphasizing an excellent scattering ability compared to dielectric compounds. We pay attention to only noble metals such as gold (Au) and silver (Ag) with LSPR in the visible range, where most random lasers studied thus far operate. Then we mention an operation principle of random lasers and application of metal nanoparticles to the random lasers. Some representative work, as well as our studies, are reviewed. In the last part, we sum up the highlight and make a brief comment on a recently demonstrated surface-plasmon-based nanolaser, in which a single nanoparticle works as a cavity.

♦ Scattering Properties of a Metal Nanoparticle

When a particle is illuminated with an electromagnetic wave, electric charges in the particle are forced into oscillatory motion by the electric field of the incident wave. The electric charges accelerated can radiate electromagnetic energy; this is a process called scattering.[3] Alternatively, absorption is a process in which the excited elementary charges transform the incident electromagnetic energy into other forms such as thermal energy. A sum of scattering and absorption is defined as extinction, which is equal to the energy given by the original incident beam. The scattering strength of a particle is evaluated by scattering cross section, σ_s, which is defined such that the total energy scattered by a particle is equal to the energy of the original beam incident on the area σ_s. A large σ_s means a strong scattering. In a similar way, absorption cross section σ_a is defined such that the energy absorbed by the particle is equal to the energy incident on the area σ_a.

The extinction properties of a metal nanoparticle around the resonance vary with the particle size. Let us briefly summarize a general tendency in size effect on the contribution of scattering and absorption.[4,5] For metal nanoparticles of less than 20 nm in diameter, absorption dominates the extinction while scattering is negligible. LSPR excited on a particle decays nonradiatively through excitation of electron–hole pairs either by intraband transitions within the conduction band or by interband transitions between filled and conduction bands. On the other hand, scattering effects are important only for nanoparticles of more than 30 nm in diameter, where electrons are accelerated due to the electromagnetic field and then radiate energy in all directions. For larger nanoparticles, scattering dominates in the extinction process, and resonance frequency shifts with increasing diameter. This means that the scattering properties can be tuned by controlling the size of nanoparticle.

Mr. Shunsuke Murai,[1] Prof. Koji Fujita,[1,2] Dr. Xiangeng Meng,[1] and Prof. Katsuhisa Tanaka*[1]*
[1]*Department of Material Chemistry, Graduate School of Engineering, Kyoto University, Katsura, Nishikyo-ku, Kyoto 615-8510*
[2]*PRESTO, Japan Science and Technology Agency (JST), 4-1-8 Honcho, Kawaguchi 332-0012*
E-mail: tanaka@dipole7.kuic.kyoto-u.ac.jp, fujita@dipole7.kuic.kyoto-u.ac.jp

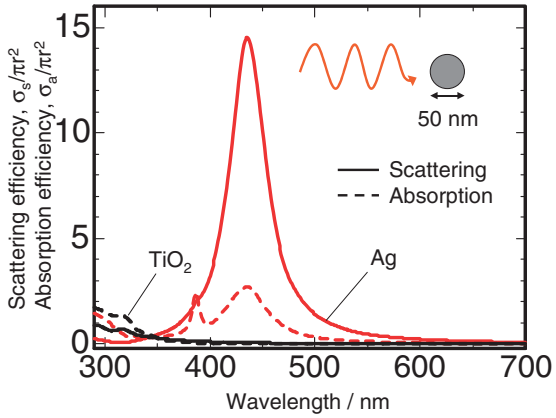

Figure 1. Extinction efficiencies calculated using Mie theory for a sphere (diameter: 50 nm) of Ag (indicated by red curves) and TiO_2 (black) embedded in a matrix with a refractive index of 1.5. Scattering and absorption efficiencies are denoted by solid and dashed curves, respectively.

To demonstrate a stronger scattering at around the LSPR frequency, the extinction properties for a nanoparticle of Ag are calculated for visible light range and compared with those for a nanoparticle of titanium dioxide (TiO_2), one of the oxides having the highest refractive index in the visible range (Figure 1). In the simulation, a sphere of Ag or TiO_2 is placed in a matrix having a refractive index of 1.5, and the scattering and absorption efficiencies, i.e., the ratios of σ_s and σ_a to the geometric cross section, are calculated based on Mie theory using a software *Mieplot*.[6] In curves for an Ag nanoparticle, two peaks appear at around 436 and 386 nm, which are ascribed to the dipole and quadrupole modes of LSPR of an Ag nanoparticle, respectively. A comparison of the scattering efficiency between TiO_2 and Ag nanoparticles clarifies that an Ag nanoparticle scatters light more efficiently, especially in the LSPR frequency range.

♦ Random Lasers

Light traveling through a system where nanoparticles are randomly dispersed undergoes scattering and interference. The scattering strength is evaluated by the scattering mean free path, the average length between two scattering events, which is expressed as

$$\ell_s = 1/\rho\sigma_s \quad (1)$$

where ρ is the number density of nanoparticles.[3] The scattering strength of a system is classified by the relation between ℓ_s and sample size L. When $\ell_s > L$, a photon on average is scattered less than one time before exiting the sample, meaning that the system is in subdiffusive or ballistic regime. In contrast, multiple scattering dominates when $\ell_s < L$, called diffusive regime where diffusion approximation explains the photon transport suitably. In the case of an extremely strong scattering system where ℓ_s is smaller than the reciprocal wave vector, i.e., $k\ell_s \leq 1$, photon localization can be established.[7] Such localization is referred to as Anderson localization of light, in analogous to localization of electrons in disordered electronic systems.[8]

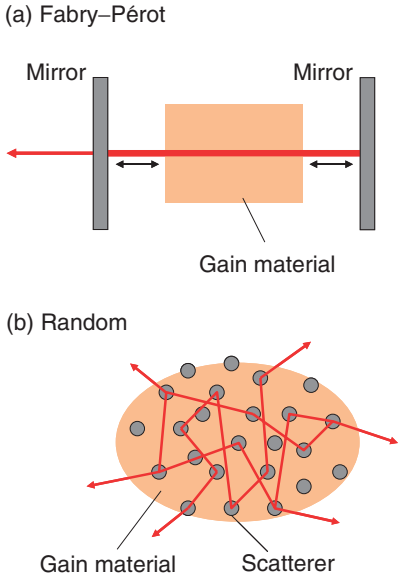

Figure 2. (a) Schematic illustration of a Fabry–Pérot laser consisting of two mirrors and a gain material. Light is confined between two mirrors, one of which partially transmits the light. (b) Effective laser cavity consisting of random distribution of scatterers with a gain material.

A random laser is realized when a gain is introduced into such a scattering medium.[9] In a random laser, multiple light scattering and interference provide an optical feedback instead of a standard Fabry–Pérot optical cavity, which is made of two mirrors (one of which partially transmits the light) that are placed to face each other on both sides of the gain material (Figure 2a). Light that is confined in the cavity interferes constructively and is amplified selectively before it escapes from the cavity through the partially transmitting mirror. When the optical amplification is large enough to compensate for the loss due to mirror leakage and material absorption, lasing oscillations occur with a well-defined frequency, good directionality, and a high degree of coherence. Although random laser works on the same principle as Fabry–Pérot lasers, the lasing modes are not determined by a predefined laser cavity but by multiple scattering. An effective cavity formed by scatterers in a volume of a random medium is a three-dimensional resonator with losses (Figure 2b). In such a cavity, the number of modes per optical frequency can be very large, and a large fraction of these modes can be nondegenerate. This leads to an overlap of their frequency spectra, and the spectrum becomes a continuum. As a consequence, emission experimentally observed manifests a smooth narrowing of the spectrum as the pump energy is increased, which can be described in terms of a simplified model of light diffusion with a gain as originally discussed by Letokhov.[10] This type of random laser is conventionally referred to as incoherent random laser.

By reducing the number of modes excited simultaneously, observation of spectrally resolved emission peaks from different modes becomes possible. This can be achieved by preparing a medium that operates in scattering regime close to localization, exciting a medium with a very small spot or using a short excitation pulse (shorter than the lifetime of the gain material).

These random lasers with discrete spectral peaks are conventionally called coherent random lasers, and many models[11] have been proposed as the origin of lasing modes, such as localized photonic modes induced by Anderson localization,[12] whispering gallery-type modes supported by randomly distributed microresonators[13] and extended modes where spontaneously emitted photons follow exceptionally long optical paths in a gain volume and eventually lase.[14]

Experimentally, coherent and incoherent random lasers have been developed using various systems with scattering strengths from nearly localized[12,15,16] to close to ballistic.[14,17] Typical forms include nanoparticles [e.g., TiO_2[18] and zinc oxide (ZnO)[19]] dispersed in dye solution and in polymer, porous monoliths [gallium phosphide (GaP)[16] and silicon dioxide (SiO_2)[20]] infiltrated with dye solution, polycrystalline semiconductor (ZnO) powders and films,[12,15] and ground laser crystals [neodymium-doped lanthanum oxide (Nd^{3+}:La_2O_3),[21] neodymium lanthanum pentaphosphate ($Nd_xLa_{1-x}P_5O_{14}$)[22]]. Numerical works have been also carried out by utilizing a finite-difference time-domain (FDTD) method in combination with the rate equations of a four-level atomic system to simulate the wave propagation in scattering media with a gain.[23]

The application of random lasers is proposed based on their properties different from those of regular lasers.[9] Low contrast of a speckle pattern of incoherent random laser is beneficial for application where homogeneous light field is required, including photolithography, display, and lighting system.[24] Meanwhile, narrow-linewidth emission of coherent random lasers is applicable for example to high-resolution wavelength-domain photonic codes and tags, which can be embedded in textile and books.[25]

♦ Random Lasers Mediated by Localized Surface Plasmon Resonance

In contrast to dielectric nanoparticles, it is only recently that metal nanoparticles have begun to be used as scatteres in random lasers in spite of their potential excellent scattering properties due to the LSPR. The first example of a metal-nanoparticle-based random laser was demonstrated in 2005 by Dice et al.[26] They prepared a rhodamine 6G (R6G) dye solution containing Ag nanoparticles (diameter: ca. 55 nm) and observed a spectral line narrowing down to 5 nm by exciting the system with 532 nm pulses from a nanosecond Nd^{3+}-doped yttrium aluminum garnet (Nd^{3+}:YAG) laser. They examined emission properties of suspensions with a various volume fraction of Ag nanoparticles and found that the sample with volume fraction of 1.5×10^{-2} vol % ($\ell_s = 1.05$ mm) had the lowest threshold. The threshold increased rapidly when the volume fraction was further increased, indicating that the absorption by Ag nanoparticles of 55 nm is not negligible. The paper points out the enhancement in dye fluorescence resulting from the enhanced localized electromagnetic field associated with LSPR, which was further discussed in their following paper.[27] It is also indicated that due to a large σ_s of an Ag nanoparticle, the geometric volume occupied by scatterers, which is required to construct a system with a given ℓ_s, can be greatly reduced compared to that for dielectric-based systems, providing a large volume left for a gain material to fill in. Subsequently Popov et al. performed research of the emission properties for R6G-doped poly(vinyl alcohol) (PVA) films 200 μm thick containing Au nanoparticles.[28] Similarly to the results reported by Dice et al., excitation with 532 nm pulses from a Nd^{3+}:YAG laser (10 ns width) allowed the observation of spectral narrowing down to ca. 5 nm. They examined the dependence of threshold on nanoparticle size with a fixed volume fraction of scatterers (6×10^{-3} vol %) and found the optimal size of 80 nm, where the threshold was the lowest. It was found that the threshold increased with the reduction of particle diameter.

In these preceding reports, the linewidth of emission spectrum was as narrow as 5 nm; in other words, incoherent random lasers were realized, and coherent random laser using metallic scatterers was still missing at that time. We have performed complementary works to demonstrate coherent random laser emission for metal-nanoparticle-based media using a picosecond excitation source.[29–31]

Our random laser consists of Ag nanoparticles embedded in polymer matrix doped with R6G molecules, where Ag nanoparticles were synthesized through a two-step seeded growth procedure. The average size of Ag nanoparticles is 50 nm in diameter, with a somewhat anisotropic shape (Figure 3a). The Ag nanoparticles exhibit intense LSPR signals over the whole visible wavelength range (Figure 3b). Two main peaks at 425 and 540 nm are ascribed to dipole modes excited along the two axes of anisotropic Ag nanoparticles, and a shoulder at 340 nm a quadrupole mode. The film with a thickness of 100 μm was prepared by cell casting from a chloroform solution where poly(methyl methacrylate) (PMMA) and R6G were dissolved and Ag nanoparticles were ultrasonically dispersed.

Typical volume fraction of the nanoparticles was 3×10^{-3} vol %, and ℓ_s was calculated to be 3.4 mm from eq 1 with σ_s being simulated by the Mie theory. On the other hand, absorption length ℓ_a, the distance when the intensity of light traveling the medium becomes e^{-1} of the initial value, was estimated to be 81 μm from the absorption spectrum. The relation of ℓ_s and ℓ_a ($\ell_s \gg \ell_a$) indicates that the photon transport inside the film is dominated by the absorption. Even in such a situation, the presence of nanoparticle makes notable difference in emission spectra. The film was pumped with the second harmonic wave (532 nm) of a mode-locked Nd^{3+}:YAG laser (PL2143AE, EKSPLA) with a duration of 25 ps and a typical repetition rate of 10 Hz. Excitation pulse was focused by a cylindrical lens to form stripe geometry having a typical length of 2.1 mm and width of 17 μm on the sample surface, and emission was collected with a CCD detector (Figure 3c). Figure 3d exhibits the integrated emission intensity as a function of pump energy. Above certain pump energy, the emission intensity increases nonlinearly, indicating existence of threshold for the emission. Figure 3e shows the variation of emission spectrum with the pump energy. When the pump energy is low, the emission spectrum exhibits a broad band centered at 590 nm with full width at half maximum (FWHM) of 46 nm, which can be ascribed to the spontaneous emission of R6G. As the pump energy is increased up to $E_{th} = 0.36$ μJ (corresponding to an excitation energy density of 0.14 MW mm^{-2}), a single sharp peak at 572 nm with FWHM less than 0.2 nm suddenly emerges in addition to the spontaneous emission band, indicating that a lasing occurs upon this pump energy. The lasing frequencies are found to vary with the irradiated position on the film, which is relevant to the randomness in spatial distribution

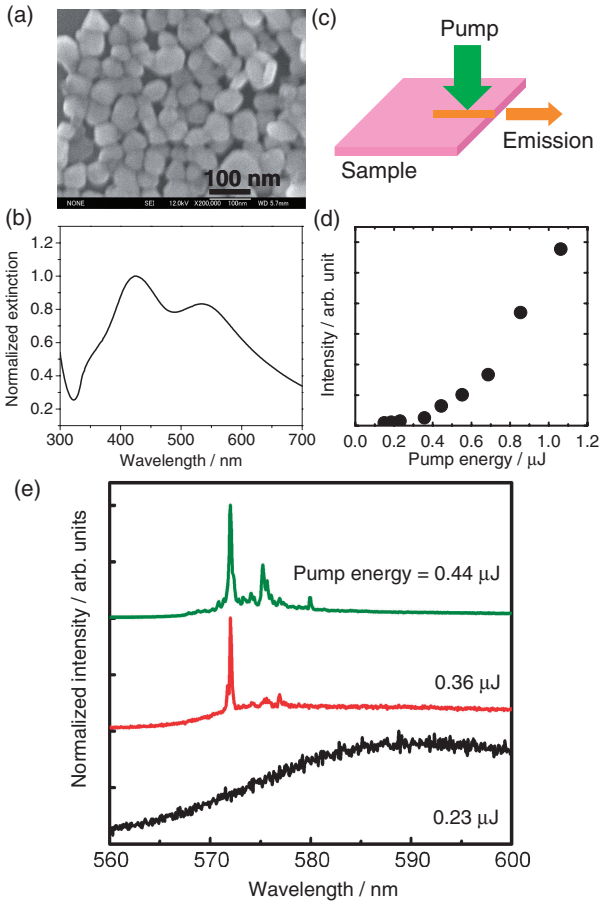

Figure 3. (a) Field emission scanning electron microscope (FE-SEM) image for Ag nanoparticles dispersed on a glass substrate. (b) Extinction spectrum of Ag nanoparticles dispersed in water, showing two main bands at 425 and 540 nm along with a shoulder at 340 nm. (c) Schematic illustration of random laser experiment showing excitation and emission configurations. (d) Dependence of integrated emission intensity on pump energy. (e) Variation of emission spectrum with pump energy. The emission spectra were obtained under pump energies of 0.23 (indicated by a black curve), 0.36 (red), and 0.44 μJ (green). The sample is a 100 μm-thick PMMA film containing 3×10^{-3} vol % Ag nanoparticles and 10 mM R6G.[30]

of Ag nanoparticles in the PMMA host. We confirmed that similar sharp emissions were still observed in the same spectral range even when the sample was excited by the third harmonic wave of the Nd^{3+}:YAG laser ($\lambda = 355$ nm). This result indicates that the observed sharp peaks are not ascribed to Raman scattering but to fluorescence. For comparison, we fabricated two kinds of dye-doped films containing TiO_2 nanoparticles (rutile-type, diameter 50 nm), one having the same ℓ_s as that for Ag-embedded film and the other having the same ρ. We also prepared a reference film containing neither Ag nor TiO_2. While a reference film without any nanoparticles merely shows a spontaneous emission band with FWHM of 46 nm under the same pumping conditions, the TiO_2-embedded films show similar random lasing with discrete emission peaks, and the thresholds ($E_{th} = 0.64$ μJ for the system with the same ℓ_s and 0.90 μJ for the same ρ) are higher than that for the Ag-embedded film.

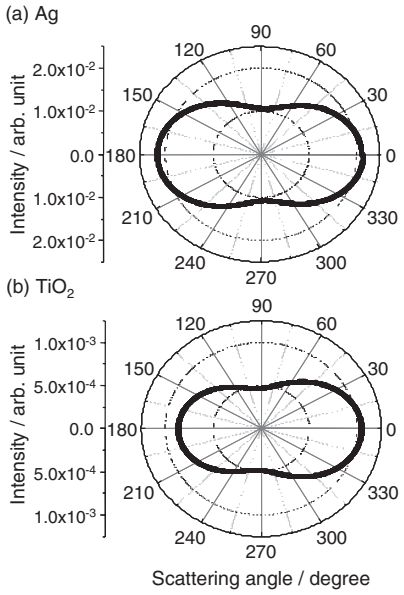

Figure 4. Angular distribution of the intensity of light scattered by a sphere with a diameter of 50 nm calculated using *Mieplot*[6] for Ag (a) and TiO_2 (b). Incident light is an unpolarized plane wave with a wavelength of 570 nm. Scattering angle of 0° corresponds to forward scattering, and 180° backscattering.

In the present system, a photon traveling inside the gain material is scattered less than one time on average before it exits because ℓ_s is longer than the excitation stripe length of 2.4 mm, meaning that the system is in subdiffusive regime. Optical amplification in this regime was discussed by Kumar et al., who proposed that the rare scattering events can significantly contribute to lasing if gain is large enough.[32] The probability that amplification occurs within the system having a size L can be described by a product of two factors, the probability that a photon is scattered back into the gain region while traveling in the system and a gain factor that a photon is amplified within the system. Let us compare the thresholds among three samples based on this discussion. When ρ is the same, both the Ag- and TiO_2-embedded films have the same gain factor because of the same volume fraction occupied by the scatterers, while the scattering probability differs from each other. The probability of backscattering is much higher for the Ag-embedded film bacause the σ_s of 50 nm Ag nanoparticles is larger by about 20 times than that of TiO_2, resulting in the lower threshold for the Ag-embedded film ($E_{th} = 0.36$ μJ) compared to the TiO_2-embedded film ($E_{th} = 0.90$ μJ). The difference in scattering strength is visualized in Figure 4, where angular distributions of the intensity of light scattered by a 50 nm Ag sphere and a TiO_2 sphere are calculated based on the Mie theory. Scattering intensity for backscattering direction (scattering angle: 180°) is far larger for Ag than TiO_2 (note that the intensity scale for the Ag nanoparticle is larger by a factor of 20 than that for the TiO_2 nanoparticle). On the other hand, when ℓ_s is the same, both the Ag- and TiO_2-embedded films have the same scattering probability, but the gain factor is different because the volume occupied by the scatterers is larger for the TiO_2-embedded sample by 20 times. This may reduce the gain for light amplification and result in the higher threshold for the TiO_2-

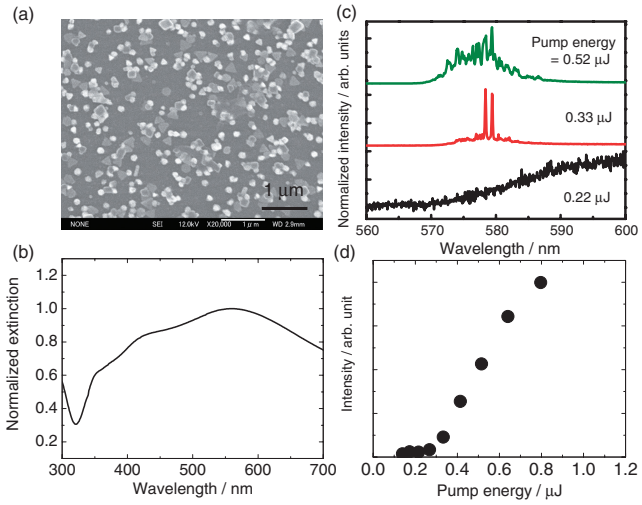

Figure 5. (a) FE-SEM image of Ag nanoprisms dispersed on a glass substrate. (b) Extinction spectrum of Ag nanoprisms suspended in an aqueous solution. (c) Emission spectra at varied pump energies for PMMA film containing Ag nanoprisms (1.2×10^{-3} vol %) and R6G (10 mM). The pump energy: 0.22 (indicated by a black curve), 0.33 (red), and 0.52 μJ (green). (d) Emission intensity as a function of pump energy.[29]

embedded film ($E_{th} = 0.64$ μJ). In addition, enhancement in localized electromagnetic field due to the LSPR can be another factor to reduce the threshold of the Ag-embedded film, although it is difficult to separate the enhancement effect from other factors and discuss quantitatively.

Progress in wet chemistry allows the fabrication of particles with a variety of morphologies. As a scatterer for random laser, we fabricated Ag nanoprisms by chemical reduction in the liquid phase (Figure 5a). Most of the Ag nanoprisms are triangular with truncated edges, with by-products of small-sized Ag nanoplates. Figure 5b shows the extinction spectrum of an aqueous suspension of Ag nanoprisms. The spectrum exhibits three bands at 351, 423, and 553 nm, corresponding to the in-plane quadrupole, out-of-plane dipole, and in-plane dipole resonances, respectively. The 100 μm-thick samples were prepared by cell-casting from a chloroform solution containing PMMA, R6G, and Ag nanoprisms. The random laser experiments were conducted with a picosecond Nd^{3+}:YAG laser using the same configuration as described in Figure 3c. Figure 5c presents the evolution of emission spectra as a function of the pump energy. The broad spontaneous emission band becomes narrow with increasing pump energy to 0.27 μJ, and narrow spikes emerge at around $\lambda = 580$ nm when the pump energy reaches 0.33 μJ, implying the onset of laser emission. The integrated intensity of emission as a function of pump energy clearly shows the existence of a threshold of laser emission (Figure 5d). The laser peaks are slightly red-shifted compared to the system containing polyhedral Ag nanoparticles shown in Figure 3e, probably reflecting a LSPR red-shift of nanoprisms.

Surprisingly, random laser action is possible even for a medium with ultrafine Ag nanoparticles, although nanoparticles less than 20 nm absorb most of the incident light and σ_s is very small. Ag nanoparticles embedded inside polymer films were prepared via in situ reduction of Ag^+. A mixture of PVA, silver nitrate, and aqueous R6G solutions was spin-coated on an SiO_2 glass substrate followed by annealing, leading to the precipitation of Ag nanoparticles with average size of 5.5 nm (Figure 6a). The random laser experiments were carried out with a picosecond Nd^{3+}:YAG laser using the same configuration as described in Figure 3c. Figure 6b depicts the evolution of emission spectra as a function of pump energy. The emission spectrum narrows down with an increase in the pump energy, and sharp spectral peaks suddenly appear at ca. 560 nm with linewidth of 0.3 nm when the pump energy reaches 1.60 μJ. At this pump energy, a film prepared without Ag nanoparticles only shows an amplified spontaneous emission (ASE) band with linewidth of 24 nm. Beyond this threshold, the emission intensity increases more rapidly and the linewidth dramatically decreases, indicating the emergence of coherent laser emissions. Compared to the σ_s for a 50 nm Ag in PVA, σ_s of 5.5 nm Ag is smaller by a factor of around 10^6 at the wavelength of emission (560 nm). This small σ_s makes ℓ_s of the system 200 mm, meaning that the film is virtually transparent because the size of the film (typically 1 cm × 1 cm × 2 μm) is much smaller than ℓ_s. We speculate that in addition to scattering, the enhancement of electromagnetic field may contribute to the appearance of sharp laser emissions.

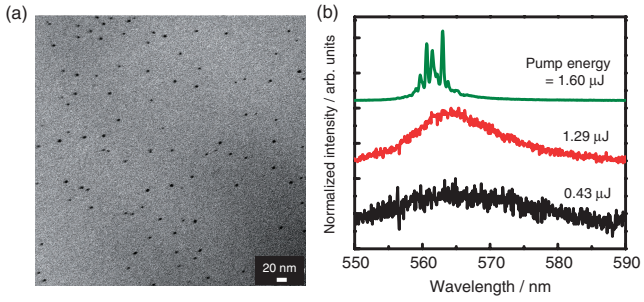

Figure 6. (a) Transmission electron microscope (TEM) image of 2 μm-thick PVA film containing Ag nanoparticles and R6G (10 mM). The average particle size is ca. 5.5 nm in diameter. (b) Emission spectra at varied pump energies. The pump energy: 0.43 (indicated by a black curve), 1.29 (red), and 1.60 (green).[31]

♦ Summary

In this review, emission properties of media based on metal nanoparticles are described after an introduction of the operation principle of random lasers. It is emphasized that a metal nanoparticle is a strong scatterer compared to a dielectric at around the frequency of LSPR, and a large σ_s of a metal nanoparticle allows fabrication of a random laser with a lower threshold compared to that containing dielectric nanoparticles. The existence of amplification effect due to the localized electromagnetic field in the vicinity of the metal surface is suggested.

As a related topic to the metal-nanoparticle-based random laser, a surface-plasmon-based nanolaser, called lasing spaser, was reported.[33,34] A spaser, abbreviation of "surface plasmon amplification by stimulated emission of radiation," is analogous to the laser. In a spaser, photons are replaced by surface plasmons, and a cavity is a nanoparticle that supports the plasmonic mode.[35] Outcoupling of surface plasmon mode to

photonic mode results in a nanolaser, which was experimentally demonstrated in a suspension of core–shell nanoparticles having an Au-core (diameter: 14 nm) and a dye-doped SiO_2 shell (thickness: 15 nm).[33] The similarity in components, i.e., a metal nanoparticle and a gain material, may allow fabrication of a spaser using the same techniques of making metal-nanoparticle-based random lasers.

This work was supported by a Grant-in-Aid for Young Scientists (B) (No. 20760451), from the Ministry of Education, Culture, Sports, Science and Technology of Japan. One of authors (X. M.) thanks the Grant-in-Aid for Fellow (No. 20-08402) from the Japan Society for the Promotion of Science (JSPS).

References and Notes

1 *Plasmonics Fundamentals and Applications*, ed. by S. A. Maier, Springer, New York, **2006**; *Princples of Nano-Optics*, ed. by L. Novotny, B. Hecht, Cambridge University Press, Cambridge, **2006**.
2 E. Ozbay, *Science* **2006**, *311*, 189; A. Polman, *Science* **2008**, *322*, 868.
3 *Absorption and Scattering of Light by Small Particles*, ed. by C. F. Bohren, D. R. Huffman, Wiley, New York, **1983**; *Light Scattering by Small Particles*, ed. by H. C. van de Hulst, Wiley, New York, **1957**.
4 C. Noguez, *Opt. Mater.* **2005**, *27*, 1204.
5 *Optical Propertes of Metal Clusters*, ed. by U. Kreibig, M. Vollmer, Springer, Berlin, **1995**.
6 P. Laven, *MIEPLOT v3.4* http://www.philiplaven.com/mieplot.htm, **2006**.
7 *Introduction to Wave Scattering, Localization, and Mesoscopic Phenomena*, ed. by P. Sheng, Academic Press, San Diego, **1995**.
8 E. Abrahams, P. W. Anderson, D. C. Licciardello, T. V. Ramakrishnan, *Phys. Rev. Lett.* **1979**, *42*, 673.
9 D. S. Wiersma, *Nat. Phys.* **2008**, *4*, 359; H. Cao, *Waves Random Media* **2003**, *13*, R1; H. Cao, *J. Phys. A: Math. Gen.* **2005**, *38*, 10497; H. Cao, *Opt. Photon. News* **2005**, *16*, 34; *Solid-State Random Lasers*, ed. by M. A. Noginov, Springer, New York, **2005**.
10 V. S. Letokhov, *Sov. Phys. JETP* **1968**, *26*, 835.
11 H. E. Türeci, L. Ge, S. Rotter, A. D. Stone, *Science* **2008**, *320*, 643.
12 H. Cao, J. Y. Xu, D. Z. Zhang, S.-H. Chang, S. T. Ho, E. W. Seelig, X. Liu, R. P. H. Chang, *Phys. Rev. Lett.* **2000**, *84*, 5584.
13 V. M. Apalkov, M. E. Raikh, B. Shapiro, *Phys. Rev. Lett.* **2002**, *89*, 016802; R. C. Polson, Z. V. Vardeny, *Phys. Rev. B* **2005**, *71*, 045205.
14 S. Mujumdar, M. Ricci, R. Torre, D. S. Wiersma, *Phys. Rev. Lett.* **2004**, *93*, 053903.
15 H. Cao, Y. G. Zhao, S. T. Ho, E. W. Seelig, Q. H. Wang, R. P. H. Chang, *Phys. Rev. Lett.* **1999**, *82*, 2278; H. Cao, Y. G. Zhao, H. C. Ong, S. T. Ho, J. Y. Dai, J. Y. Wu, R. P. H. Chang, *Appl. Phys. Lett.* **1998**, *73*, 3656.
16 K. L. van der Molen, R. W. Tjerkstra, A. P. Mosk, A. Lagendijk, *Phys. Rev. Lett.* **2007**, *98*, 143901.
17 X. Wu, W. Fang, A. Yamilov, A. A. Chabanov, A. A. Asatryan, L. C. Botten, H. Cao, *Phys. Rev. A* **2006**, *74*, 053812; S. V. Frolov, Z. V. Vardeny, K. Yoshino, A. Zakhidov, R. H. Baughman, *Phys. Rev. B* **1999**, *59*, R5284.
18 N. M. Lawandy, R. M. Balachandran, A. S. L. Gomes, E. Sauvain, *Nature* **1994**, *368*, 436; W. L. Sha, C.-H. Liu, R. R. Alfano, *Opt. Lett.* **1994**, *19*, 1922.
19 H. Cao, J. Y. Xu, S.-H. Chang, S. T. Ho, *Phys. Rev. E* **2000**, *61*, 1985.
20 S. Murai, K. Fujita, K. Nakanishi, K. Hirao, *J. Non-Cryst. Solids* **2004**, *345–346*, 438.
21 V. M. Markushev, V. F. Zolin, C. M. Briskina, *Zh. Prikl. Spektrosk.* **1986**, *45*, 847.
22 C. Gouedard, D. Husson, C. Sauteret, F. Auzel, A. Migus, *J. Opt. Soc. Am. B* **1993**, *10*, 2358.
23 X. Y. Jiang, C. M. Soukoulis, *Phys. Rev. Lett.* **2000**, *85*, 70; C. Vanneste, P. Sebbah, *Phys. Rev. Lett.* **2001**, *87*, 183903.
24 G. Williams, B. Bayram, S. C. Rand, T. Hinklin, R. M. Laine, *Phys. Rev. A* **2001**, *65*, 013807; V. S. Letokhov, S. K. Sekatskii, *Quantum Electron.* **2002**, *32*, 1007.
25 R. M. Balachandran, D. P. Pacheco, N. M. Lawandy, *Appl. Opt.* **1996**, *35*, 640; R. M. Balachandran, D. P. Pacheco, N. M. Lawandy, Conference on Lasers and Electro-Optics, OSA Technical Digest Series, Washington D. C., **1995**, Vol. 15, p. 114.
26 G. D. Dice, S. Mujumdar, A. Y. Elezzabi, *Appl. Phys. Lett.* **2005**, *86*, 131105.
27 G. D. Dice, A. Y. Elezzabi, *J. Opt. A: Pure Appl. Opt.* **2007**, *9*, 186.
28 O. Popov, A. Zilbershtein, D. Davidov, *Appl. Phys. Lett.* **2006**, *89*, 191116.
29 X. Meng, K. Fujita, S. Murai, K. Tanaka, *J. Jpn. Soc. Powder Powder Metall.* **2009**, *56*, 645.
30 X. Meng, K. Fujita, S. Murai, K. Tanaka, *Phys. Rev. A* **2009**, *79*, 053817.
31 X. Meng, K. Fujita, Y. Zong, S. Murai, K. Tanaka, *Appl. Phys. Lett.* **2008**, *92*, 201112; X. Meng, K. Fujita, S. Murai, Y. Zong, S. Akasaka, H. Hasegawa, K. Tanaka, *Phys. Status Solidi C* **2009**, *6*, S102.
32 B. R. Prasad, H. Ramachandran, A. K. Sood, C. K. Subramanian, N. Kumar, *Appl. Opt.* **1997**, *36*, 7718.
33 M. A. Noginov, G. Zhu, A. M. Belgrave, R. Bakker, V. M. Shalaev, E. E. Narimanov, S. Stout, E. Herz, T. Suteewong, U. Wiesner, *Nature* **2009**, *460*, 1110.
34 N. I. Zheludev, S. L. Prosvirnin, N. Papasimakis, V. A. Fedotov, *Nat. Photonics* **2008**, *2*, 351.
35 D. J. Bergman, M. I. Stockman, *Phys. Rev. Lett.* **2003**, *90*, 027402.

